Geometric Information Field Theory

Topological Derivation of Standard Model Parameters from G_2 Holonomy Manifolds

---

Version: 3.3

Author: Brieuc de La Fournière

Independent researcher, Beaune, France

Abstract

The Standard Model's 19 free parameters lack theoretical explanation. We explore a geometric framework in which these parameters emerge as algebraic combinations of topological invariants of a seven-dimensional G_2 holonomy manifold K_7 coupled to $E_8 \times E_8$ gauge structure, with zero continuous adjustable parameters.

The framework rests on three elements: (i) a compact G_2 manifold with Betti numbers $b_2 = 21$, $b_3 = 77$ (plausible within the twisted connected sum landscape); (ii) a dynamical mechanism in which torsion of the G_2 3-form drives geodesic flow on K_7, identified with renormalization group evolution; and (iii) scale determination through topological exponents, yielding the electron mass at 0.09% and the electroweak scale at 0.4% (status: THEORETICAL). From these inputs, 33 dimensionless predictions follow with mean deviation **0.24%** across 32 well-measured observables, including the Koide parameter $Q = 2/3$, the neutrino CP phase $\delta_{CP} = 197°$ (within 1σ of NuFIT 6.0), and the dark-to-baryonic matter ratio $\Omega_{DM}/\Omega_b = 43/8$. Including δ_{CP} (whose experimental uncertainty is $\pm 11\%$) raises the mean to 0.57%. Of the 33, 18 core relations are algebraically verified in Lean 4.

Statistical analysis confirms uniqueness at multiple levels: $(b_2, b_3) = (21, 77)$ outperforms all 3,070,396 tested alternatives including 30 known G_2 manifolds ($p < 2 \times 10^{-5}$), remains the unique optimum under leave-one-out cross-validation (28/28), and joint null models reject accidental matching at $p < 10^{-5}$ without independence assumptions, confirmed by Bayesian analysis (Bayes factors 288–4,567) and Westfall–Young correction (11/33 individually significant, global $p = 0.008$). The Deep Underground Neutrino Experiment (DUNE, 2028–2040) provides a decisive test: measurement of δ_{CP} outside 182°–212° would refute the framework. We present this as an exploratory investigation emphasizing falsifiability, not a claim of correctness.

Keywords: G_2 holonomy, exceptional Lie algebras, Standard Model parameters, topological field theory, falsifiability, formal verification

---

"A theory with mathematical beauty is more likely to be correct than an ugly one that fits some experimental data."
– Paul Dirac

Contents

1 Introduction

1.1 The Parameter Problem

The Standard Model describes fundamental interactions with remarkable precision, yet requires 19 free parameters determined solely through experiment [1]. These parameters (gauge couplings, Yukawa couplings spanning five orders of magnitude, mixing matrices, and Higgs sector values) lack theoretical explanation.

Several tensions motivate the search for deeper structure:

- **Hierarchy problem**: The Higgs mass requires fine-tuning absent new physics [2].
- **Hubble tension**: CMB and local H_0 measurements differ by $> 4\sigma$ [3, 4].
- **Flavor puzzle**: No mechanism explains three generations or mass hierarchies [5].
- **Koide mystery**: The charged lepton relation $Q = 2/3$ holds for 43 years without explanation [6].

These challenges suggest examining whether parameters might emerge from geometric or topological structures.

1.2 Contemporary Context

The present framework connects to three active research programs:

Division algebra program (Furey, Hughes, Dixon [7, 8]): Derives Standard Model symmetries from the tensor product of complex numbers and octonions. GIFT adds compactification geometry and numerical predictions.

$E_8 \times E_8$ **unification**: Wilson (2024) shows $E_8(-248)$ encodes three fermion generations with Standard Model gauge structure [9]. Singh, Kaushik et al. (2024) develop similar $E_8 \times E_8$ unification [10]. GIFT extracts numerical values from this structure.

G_2 **holonomy physics** (Acharya, Haskins, Foscolo–Nordström [11, 12, 13]): M-theory on G_2 manifolds. Recent work (2022–2025) extends twisted connected sum constructions [14, 15]. Crowley, Goette, and Nordström (Inventiones 2025) prove the moduli space of G_2 metrics is disconnected [13]. GIFT derives dimensionless constants from topological invariants.

1.3 Framework Overview

The Geometric Information Field Theory (GIFT) proposes that dimensionless parameters represent topological invariants of an eleven-dimensional spacetime:

```
E8 x E8 (496D) --> AdS4 x K7 (11D) --> Standard Model (4D)
```

The key elements:

1. $E_8 \times E_8$ **gauge structure** (dimension 496)
2. **Compact 7-manifold** K_7 with G_2 holonomy ($b_2 = 21$, $b_3 = 77$)
3. **Model normalization** of the G_2 metric ($\det(g) = 65/32$)
4. **Cohomological mapping**: Betti numbers constrain field content

We emphasize this represents mathematical exploration, not a claim that nature realizes this structure. The framework's merit lies in falsifiable predictions from topological inputs.

1.4 Paper Organization

- Section 2: Mathematical framework ($E_8 \times E_8$, K_7, G_2 structure)
- Section 3: Physical mechanism: torsion and RG flow
- Section 4: Methodology and epistemic status
- Section 5: Derivation of 33 dimensionless predictions
- Section 6: Scale determination and dimensional predictions
- Section 7: Formal verification and statistical analysis
- Section 8: The G_2 metric program
- Section 9: Falsifiable predictions
- Section 10: Discussion and limitations
- Section 11: Conclusion

Technical details of the E_8 and G_2 structures appear in Supplement S1: Mathematical Foundations. Complete derivation proofs for all 18 verified relations appear in Supplement S2: Complete Derivations.

2 Mathematical Framework

2.1 The Octonionic Foundation

GIFT emerges from the algebraic fact that **the octonions are the largest normed division algebra**.

Algebra	Dim	Physics Role	Extends?
$\mathbb{R}$	1	Classical mechanics	Yes
$\mathbb{C}$	2	Quantum mechanics	Yes
$\mathbb{H}$	4	Spin, Lorentz group	Yes
$\mathbb{O}$	**8**	**Exceptional structures**	**No**

The octonions terminate this sequence. Their automorphism group $G_2 = \mathrm{Aut}(\mathbb{O})$ has dimension 14 and acts naturally on $\mathrm{Im}(\mathbb{O}) = \mathbb{R}^7$. The exceptional Lie algebras arise from octonionic constructions through a chain established by Dray and Manogue [16]:

Algebra	Dimension	Connection to $\mathbb{O}$
G_2	14	$\mathrm{Aut}(\mathbb{O})$
F_4	52	$\mathrm{Aut}(J_3(\mathbb{O}))$
E_6	78	Collineations of $\mathbb{O}P^2$
E_8	248	Contains all lower exceptionals

This chain is not accidental. It reflects the unique algebraic structure of the octonions: $\mathrm{Im}(\mathbb{O})$ has dimension 7, the Fano plane encodes the multiplication table, and G_2 preserves this structure. A G_2-holonomy manifold is therefore the natural geometric home for octonionic physics, just as U(1) holonomy is the natural setting for complex geometry.

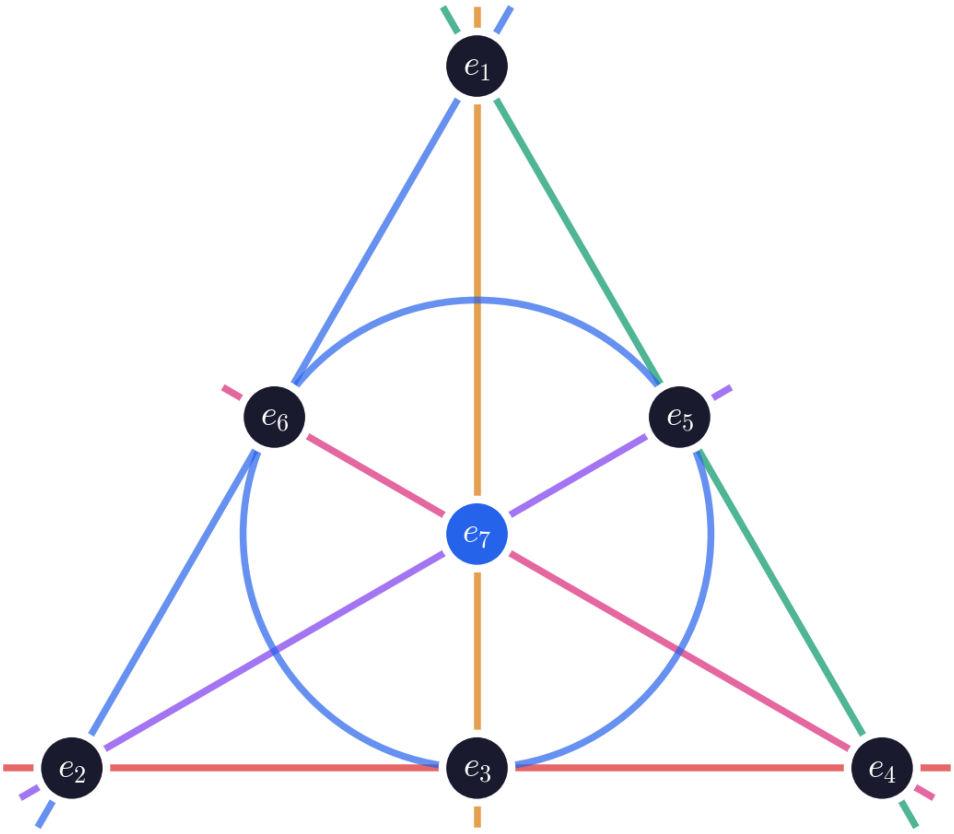

Figure 1: The Fano plane encoding the octonion multiplication table. Each line (including the circle) represents a quaternionic triple.

2.2 $E_8 \times E_8$ Structure

E_8 is the largest exceptional simple Lie group with dimension 248 and rank 8 [17]. The product $E_8 \times E_8$ arises in heterotic string theory for anomaly cancellation [18], with total dimension 496.

The first E_8 contains the Standard Model gauge group through the breaking chain:

```
E8 --> E6 x SU(3) --> SO(10) x U(1) --> SU(5) --> SU(3) x SU(2) x U(1)
```

The second E_8 provides a hidden sector whose physical interpretation remains an open question.

Wilson (2024) demonstrates that $E_8(-248)$ encodes three fermion generations (128 degrees of freedom) with GUT structure [9]. The product dimension 496 enters the hierarchy parameter $\tau = (496 \times 21)/(27 \times 99) = 3472/891$, connecting gauge structure to internal topology.

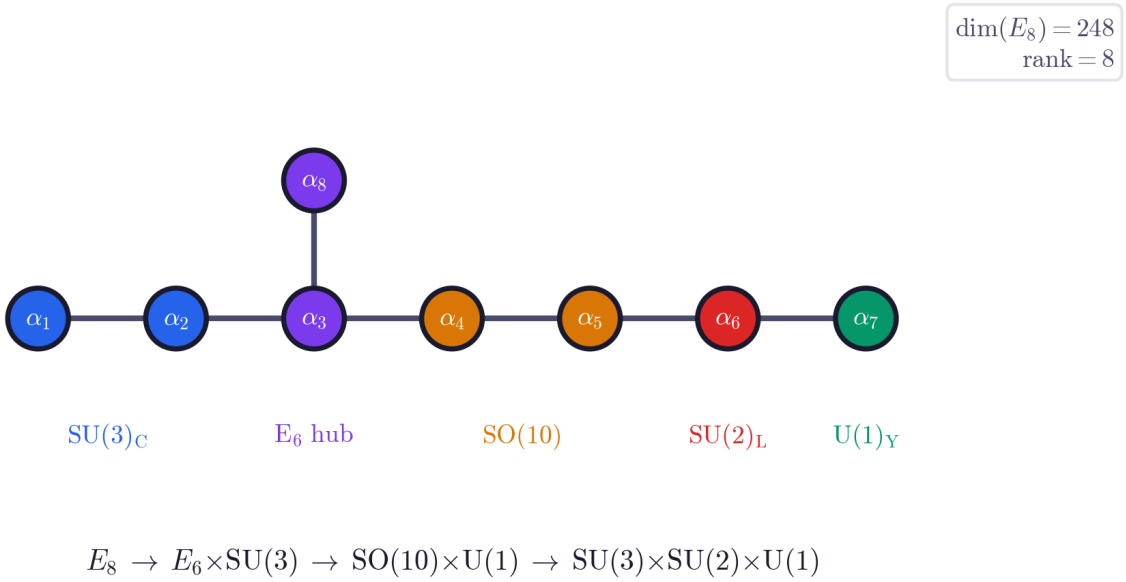

Figure 2: The E_8 Dynkin diagram. The 8 nodes correspond to simple roots; the extended structure encodes the 240-root system.

2.3 The K_7 Manifold Hypothesis

2.3.1 Statement of Hypothesis

Hypothesis: There exists a compact 7-manifold K_7 with G_2 holonomy satisfying:

- Second Betti number: $b_2(K_7) = 21$
- Third Betti number: $b_3(K_7) = 77$
- Simple connectivity: $\pi_1(K_7) = 0$

We do not claim to have constructed such a manifold explicitly. Rather, we assume its existence and derive consequences from these topological data.

2.3.2 Plausibility from TCS Constructions

The twisted connected sum (TCS) method of Joyce [19] and Kovalev [20], extended by Corti–Haskins–Nordström–Pacini [21] and recent work on extra-twisted connected sums [14, 15], produces compact G_2 manifolds with controlled Betti numbers.

TCS constructions glue two asymptotically cylindrical building blocks:

$$K_7 = M_1^T \cup_\varphi M_2^T$$

Proposed building blocks for K_7:

Region	Construction	b_2	b_3
M_1	Quintic in $\mathbb{CP}^4$	11	40
M_2	CI(2,2,2) in $\mathbb{CP}^6$	10	37
K_7	**TCS gluing**	**21**	**77**

For such building blocks, the Betti numbers would follow from the Mayer–Vietoris sequence:

- $b_2(K_7) = b_2(M_1) + b_2(M_2) = 11 + 10 = 21$
- $b_3(K_7) = b_3(M_1) + b_3(M_2) = 40 + 37 = 77$

We do not cite a specific construction achieving exactly these values with all required properties; however, such manifolds are plausible within the TCS/ETCS landscape.

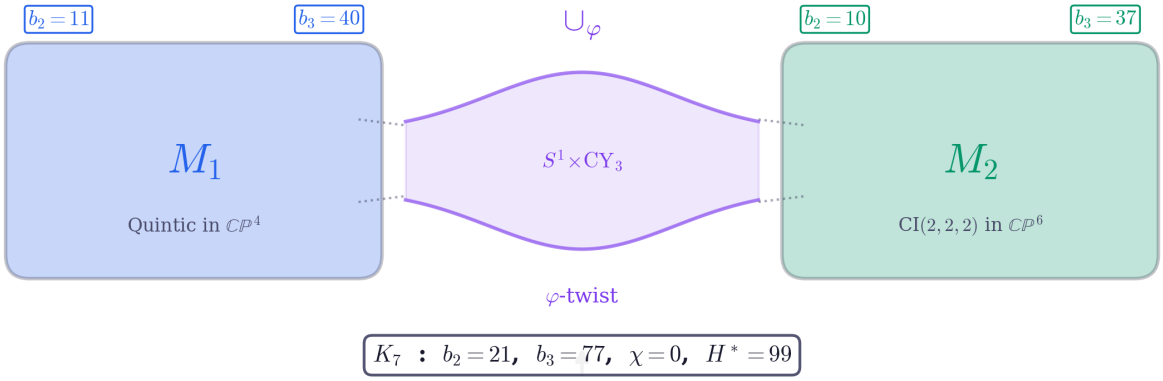

Figure 3: Twisted connected sum construction of K_7. Two asymptotically cylindrical building blocks M_1 and M_2 are glued along their cylindrical ends via a twist diffeomorphism.

The cohomological sum:

$$H^* = b_2 + b_3 + 1 = 21 + 77 + 1 = 99$$

The Euler characteristic vanishes by Poincaré duality for any compact oriented odd-dimensional manifold:

$$\chi(K_7) = 1 - 0 + 21 - 77 + 77 - 21 + 0 - 1 = 0$$

2.3.3 G_2 Holonomy: Why This Choice

G_2 holonomy occupies a special position in Berger's classification. It appears only in dimension seven and has three properties relevant to physics:

- **Supersymmetry preservation**: Compactification on a G_2 manifold preserves exactly $N = 1$ SUSY in 4D [11].
- **Ricci-flatness**: G_2 holonomy implies $\mathrm{Ric}(g) = 0$, solving the vacuum Einstein equations.
- **Exceptional structure**: $G_2 = \mathrm{Aut}(\mathbb{O})$ is not a choice but a mathematical identity. The 7 imaginary octonion units span $\mathrm{Im}(\mathbb{O}) = \mathbb{R}^7$, and G_2 preserves the octonionic multiplication table.

This addresses the selection principle question: K_7 is not chosen from a landscape of alternatives. It is a geometric realization of octonionic structure, suggested by the division algebra chain. We do not claim uniqueness; we claim this is the setting suggested by the mathematics.

2.4 G_2 Structure and Metric Constraints

2.4.1 The Standard G_2 Form

On the tangent space $T_pK_7 = \mathbb{R}^7$, the G_2 structure is locally modeled by the standard associative 3-form of Harvey–Lawson [22]:

$$\varphi_0 = e^{123} + e^{145} + e^{167} + e^{246} - e^{257} - e^{347} - e^{356}$$

This form has 7 non-zero components among $\binom{7}{3} = 35$ basis elements and defines a metric $g_0 = I_7$ with induced volume form. G_2 holonomy is equivalent to existence of a parallel 3-form satisfying $d\varphi = 0$ and $d{*}\varphi = 0$, where $*$ denotes Hodge duality.

2.4.2 Model Normalization on the Metric Determinant

We impose a model-level normalization on the global volume scale of the G_2 metric:

$$\det(g) = \frac{65}{32}$$

This value is expressed in terms of topological integers:

$$\det(g) = p_2 + \frac{1}{b_2 + \dim(G_2) - N_{\text{gen}}} = 2 + \frac{1}{32} = \frac{65}{32}$$

This is **not** claimed to be a topological invariant; it is a defining constraint of the framework, fixing an overall normalization (choice of scale) for the reference G_2 structure. To realize $\det(g) = 65/32$, the standard associative 3-form is scaled by $c = (65/32)^{1/14} \approx 1.054$. The role of $\varphi_{\text{ref}} = c \cdot \varphi_0$ is purely algebraic and local: the canonical G_2 structure in a local orthonormal coframe.

Important: φ_{ref} is not proposed as a globally constant solution on K_7. The actual torsion-free solution has the form $\varphi = \varphi_{\text{ref}} + \delta\varphi$, with global closure and co-closure constraints ($d\varphi = 0$, $d{*}\varphi = 0$) established by Joyce's theorem.

2.4.3 Torsion-Free Existence

The torsion parameter, characterizing the manifold's structure:

$$\kappa_T = \frac{1}{b_3 - \dim(\mathrm{G}_2) - p_2} = \frac{1}{77 - 14 - 2} = \frac{1}{61}$$

where $p_2 = \dim(\mathrm{G}_2)/\dim(K_7) = 2$. Joyce's theorem [19] guarantees existence of a torsion-free G_2 metric when the torsion norm is below a threshold. PINN validation (Section 8) confirms the norm remains well within this regime, with a safety margin exceeding two orders of magnitude.

Robustness of predictions: The 33 dimensionless predictions derive from topological invariants (b_2, b_3, $\dim(\mathrm{G}_2)$, etc.) that are independent of the specific realization of $\delta\varphi$. The predictions depend only on topology, not on the detailed geometry of the torsion-free metric.

2.5 Topological Constraints on Field Content

2.5.1 Betti Numbers as Capacity Bounds

The Betti numbers provide upper bounds on field multiplicities:

- $\mathbf{b_2(K_7) = 21}$: Bounds the number of gauge field degrees of freedom
- $\mathbf{b_3(K_7) = 77}$: Bounds the number of matter field degrees of freedom

Important caveat: On a smooth G_2 manifold, dimensional reduction yields b_2 abelian U(1) vector multiplets [11]. Non-abelian gauge groups (such as $\mathrm{SU}(3) \times \mathrm{SU}(2) \times \mathrm{U}(1)$) require singularities in the G_2 manifold, specifically codimension-4 singularities with ADE-type structure [23, 24]. We assume K_7 admits such singularities; a complete treatment would require specifying the singular locus.

2.5.2 Generation Number

The number of chiral fermion generations follows from a topological constraint:

$$(\mathrm{rank}(\mathrm{E}_8) + N_{\mathrm{gen}}) \times b_2 = N_{\mathrm{gen}} \times b_3$$

Solving: $(8 + N_{\mathrm{gen}}) \times 21 = N_{\mathrm{gen}} \times 77$ yields $\mathbf{N_{gen} = 3}$.

This derivation is formal; physically, it reflects index-theoretic constraints on chiral zero modes, which in M-theory on G_2 require singular geometries for chirality [24].

3 Physical Mechanism: Torsion and RG Flow

Sections 2.1–2.4 establish the static topological data of K_7. A persistent question is: how do topological integers become physical coupling constants? The bridge is **torsion**: the failure of the G_2 3-form to be parallel. This section develops the dynamical framework connecting static topology to physical evolution.

3.1 Torsion as Source of Interactions

On a torsion-free G_2 manifold ($d\varphi = 0$, $d{*}\varphi = 0$), different sectors of the geometry decouple: there are no interactions. Physical interactions require controlled departure from the torsion-free condition:

$$|d\varphi|^2 + |d{*}\varphi|^2 = \kappa_T^2, \quad \kappa_T = \frac{1}{b_3 - \dim(G_2) - p_2} = \frac{1}{61}$$

The non-closure of φ is not a defect but a feature: it provides the geometric mechanism through which particle sectors interact.

3.2 Torsion Class Decomposition

On a 7-manifold with G_2 structure, the intrinsic torsion decomposes into four irreducible G_2 representations:

$$T \in W_1 \oplus W_7 \oplus W_{14} \oplus W_{27}$$

Class	Dimension	Characterization
W_1	1	Scalar: $d\varphi = \tau_0 \star \varphi$
W_7	7	Vector: $d\varphi = 3\tau_1 \wedge \varphi$
W_{14}	14	Co-closed part of $d{\star}\varphi$
W_{27}	27	Traceless symmetric

Total dimension: $1 + 7 + 14 + 27 = 49 = \dim(K_7)^2$. This decomposition constrains which physical sectors interact and at what strength. The torsion-free condition requires all four classes to vanish simultaneously.

3.3 Torsional Geodesic Equation

Curves $x^k(\lambda)$ on K_7 satisfy the geodesic equation with torsionful connection. For the metric-compatible connection with contorsion $K_{ij}^k = \frac{1}{2}T_{ij}^k$, the variational principle yields:

$$\boxed{\frac{d^2x^k}{d\lambda^2} = \frac{1}{2}g^{kl}T_{ijl}\frac{dx^i}{d\lambda}\frac{dx^j}{d\lambda}}$$

This is the central dynamical equation: acceleration along geodesics arises from torsion, with quadratic velocity dependence. The equation preserves the kinetic energy invariant $E = g_{ij}(dx^i/d\lambda)(dx^j/d\lambda) = \text{const}$.

3.4 RG Flow Identification

The identification $\lambda = \ln(\mu/\mu_0)$ maps geodesic flow to renormalization group evolution:

Geometric quantity	Physical quantity
Position $x^k(\lambda)$	Coupling constant value
Parameter λ	RG scale $\ln(\mu)$
Velocity $dx^k/d\lambda$	Beta-function β^k
Acceleration $d^2x^k/d\lambda^2$	Beta-function derivative
Torsion T_{ijl}	Interaction kernel

The structural parallel is precise: both are one-parameter flows on a coupling manifold governed by nonlinear ODEs with quadratic velocity dependence. Fixed points in both frameworks correspond to conformal field theories. Whether this correspondence reflects a deeper mathematical equivalence or an effective description remains an open question.

3.5 Ultra-Slow Flow and Experimental Compatibility

Experimental bounds from atomic clock experiments constrain the time variation of fundamental constants to $|\dot{\alpha}/\alpha| < 10^{-17}$ yr^{-1}. The geodesic flow velocity satisfies:

$$\frac{\dot{\alpha}}{\alpha} \sim H_0 \times |\Gamma| \times |v|^2$$

With $H_0 \sim 3.0 \times 10^{-18}$ s^{-1} and $|\Gamma| \sim \kappa_T / \det(g) \sim 0.008$, the constraint requires $|v| < 0.7$. The framework value $|v| \sim 0.015$ satisfies this with large margin, yielding $|\dot{\alpha}/\alpha| \sim 10^{-16}$ yr^{-1}.

DESI DR2 compatibility: The cosmological bound $|T|^2 < 10^{-3}$ (95% CL) is satisfied by $\kappa_T^2 = 1/3721 \approx 2.7 \times 10^{-4}$.

3.6 Torsion Hierarchy and Observable Hierarchy

Numerical reconstruction of the torsion tensor on K_7 reveals three components spanning five orders of magnitude:

Component	Magnitude	Physical Role
$T_{e,\varphi,\pi}$	~ 5	Mass hierarchies (large ratios)
$T_{\pi,\varphi,e}$	~ 0.5	CP violation phase
$T_{e,\pi,\varphi}$	$\sim 3 \times 10^{-5}$	Jarlskog invariant

The torsion hierarchy directly encodes the observed hierarchy of physical observables: the mass ratio $m_\tau/m_e = 3477$ arises from large torsion in the (e, φ) plane, the CP phase $\delta_{\text{CP}} = 197°$ from moderate torsion in the (π, φ) sector, and the Jarlskog invariant $J \sim 3 \times 10^{-5}$ from the tiny component $T_{e,\pi,\varphi}$.

4 Methodology and Epistemic Status

4.1 The Derivation Principle

The GIFT framework derives physical observables through algebraic combinations of topological invariants:

```
Topological Invariants --> Algebraic Combinations --> Dimensionless Predictions
     (exact integers)        (symbolic formulas)        (testable quantities)
```

Three classes of predictions emerge:

1. **Structural integers**: Direct topological consequences. Example: $N_{\text{gen}} = 3$ from the index theorem.
2. **Exact rationals**: Simple algebraic combinations yielding rational numbers. Example: $\sin^2\theta_W = 21/91 = 3/13$.
3. **Algebraic irrationals**: Combinations involving transcendental functions that nonetheless derive from geometric structure. Example: $\alpha_s = \sqrt{2}/12$.

4.2 What GIFT Claims and Does Not Claim

Inputs (hypotheses):

- Existence of K_7 with G_2 holonomy and $(b_2, b_3) = (21, 77)$
- $\mathrm{E}_8 \times \mathrm{E}_8$ gauge structure with standard algebraic data
- Model normalization $\det(g) = 65/32$

Outputs (derived quantities):

- 33 dimensionless ratios expressed in terms of topological integers

We claim that given the inputs, the outputs follow algebraically. We do **not** claim:

1. That $\mathbb{O} \to \mathrm{G}_2 \to K_7$ is the unique geometry for physics
2. That the formulas are uniquely determined by geometric principles
3. That the selection rule for specific combinations (e.g., $b_2/(b_3 + \dim(\mathrm{G}_2))$ rather than b_2/b_3) is understood, though these formulas are statistically distinguished among alternatives (Section 7.5)
4. That dimensional quantities (masses in eV) have the same confidence as dimensionless ratios

4.3 Structural Properties of the Framework

Multiplicity: 33 independent predictions, not cherry-picked coincidences. The 32 well-measured observables (excluding δ_{CP}, whose experimental uncertainty is $\pm 11\%$) achieve 0.24% mean deviation. Even

including δ_{CP} at its face-value 11.3% discrepancy, the combined 0.57% has probability $< 2 \times 10^{-5}$ under three independent null models (permutation, structure-preserved, adversarial; 50,000 trials each).

Exactness: Several predictions are exactly rational:

- $\sin^2 \theta_W = 3/13$ (not 0.2308...)
- $Q_{\text{Koide}} = 2/3$ (not 0.6667...)
- $m_s/m_d = 20$ (not 19.8...)

These exact ratios cannot be "fitted"; they are correct or wrong.

Falsifiability: DUNE will test $\delta_{\text{CP}} = 197°$ to $\pm 5°$ precision by 2039. A single clear contradiction would strongly disfavor the framework. NuFIT 6.0 has shifted the best-fit to $177° \pm 20°$, placing the GIFT prediction at 1σ; resolution requires DUNE's precision.

4.4 The Open Question

The principle selecting these specific algebraic combinations of topological invariants remains unknown. This parallels Balmer's formula (1885) for hydrogen spectra: an empirically successful description whose theoretical derivation (Bohr, Schrödinger) came decades later. While a first quantification of the formula-level look-elsewhere effect (Section 7.5) establishes that the GIFT formulas are statistically distinguished within a bounded grammar, it does not explain *why* these combinations are optimal.

An encouraging structural observation: quantities with strong physical significance admit multiple equivalent algebraic formulations from the same topological constants. For instance, $\sin^2 \theta_W = 3/13$ can be expressed through at least 14 combinations, and $Q_{\text{Koide}} = 2/3$ through at least 20. This structural coherence suggests the values are embedded in the algebraic web of topological invariants, though the number of expressions depends on the grammar used for enumeration (Section 7.5). Complete expression counts appear in Supplement S2.

4.5 Why Dimensionless Quantities

GIFT focuses on dimensionless ratios because they depend on topology alone: the ratio $\sin^2 \theta_W = 3/13$ is the same whether masses are measured in eV, GeV, or Planck units. The torsional geodesic framework (Section 3) provides the mechanism connecting topology to scale-dependent physics by identifying geodesic flow with RG evolution, but dimensional predictions carry additional theoretical uncertainty (Section 6). The 33 dimensionless predictions stand on topology; the dynamical framework (Section 3) provides the mechanism, and the scale determination (Section 6) extends the reach to dimensional quantities.

4.6 Data Conventions

All experimental comparisons use the following conventions:

- **Electroweak mixing angle**: $\sin^2 \theta_W$ in the $\overline{\text{MS}}$ scheme at the Z pole (PDG 2024 global fit: 0.23122 ± 0.00004). The GIFT ratio $3/13 = 0.230769$ is compared to this running value.

- **Quark masses**: $\overline{\text{MS}}$ masses at $\mu = 2$ GeV for light quarks (u, d, s) and at $\mu = m_Q$ for heavy quarks (c, b, t), following PDG 2024 conventions.
- **Lepton masses**: Pole masses (PDG 2024).
- **CKM parameters**: Standard PDG parametrization with Wolfenstein convention for A, λ.
- **PMNS parameters**: NuFIT 6.0 global fit with Super-Kamiokande atmospheric data (normal ordering).
- **Cosmological parameters**: Planck 2020 (TT,TE,EE+lowE+lensing), except H_0 which uses the Planck best-fit value $h = 0.674$.
- **Strong coupling**: $\alpha_s(M_Z)$ in the $\overline{\text{MS}}$ scheme (PDG 2024: 0.1179 ± 0.0009).

Where GIFT predicts exact rationals ($\sin^2\theta_W = 3/13$, $Q_{\text{Koide}} = 2/3$), deviations from experiment may reflect radiative corrections, scheme dependence, or genuine discrepancy.

5 Derivation of the 33 Dimensionless Predictions

5.1 Gauge Sector

5.1.1 Weinberg Angle

$$\sin^2\theta_W = \frac{b_2}{b_3 + \dim(\mathrm{G}_2)} = \frac{21}{91} = \frac{3}{13} = 0.230769$$

Experimental (PDG 2024) [1]: 0.23122 ± 0.00004. Deviation: **0.195%**.

The numerator b_2 counts gauge moduli; the denominator $b_3 + \dim(\mathrm{G}_2)$ counts matter plus holonomy degrees of freedom. The ratio measures gauge-matter coupling geometrically.

5.1.2 Strong Coupling

$$\alpha_s(M_Z) = \frac{\sqrt{2}}{\dim(\mathrm{G}_2) - p_2} = \frac{\sqrt{2}}{12} = 0.11785$$

Experimental: 0.1179 ± 0.0009. Deviation: **0.04%**.

5.2 Lepton Sector

5.2.1 Koide Parameter

The Koide formula has resisted explanation since 1982. Koide discovered an empirical relation among the charged lepton masses [6]:

$$Q = \frac{(m_e + m_\mu + m_\tau)^2}{(\sqrt{m_e} + \sqrt{m_\mu} + \sqrt{m_\tau})^2} = \frac{2}{3}$$

Using contemporary mass values, this holds to six significant figures: $Q_{\text{exp}} = 0.666661 \pm 0.000007$.

GIFT provides:

$$Q_{\text{Koide}} = \frac{\dim(\text{G}_2)}{b_2} = \frac{14}{21} = \frac{2}{3}$$

The derivation requires only two topological invariants: $\dim(\text{G}_2) = 14$ (holonomy group dimension) and $b_2 = 21$ (second Betti number). No fitting is involved.

Approach	Result	Status
Preon models (Koide 1982)	$Q = 2/3$ assumed	Circular
S_3 symmetry (various)	$Q \approx 2/3$ fitted	Approximate
GIFT	$\mathbf{Q = \dim(\text{G}_2)/b_2 = 14/21 = 2/3}$	**Algebraic identity**

Deviation: 0.0009%, the smallest among all 33 predictions.

5.2.2 Tau-Electron Mass Ratio

$$\frac{m_\tau}{m_e} = \dim(K_7) + 10 \times \dim(\text{E}_8) + 10 \times H^* = 7 + 2480 + 990 = 3477$$

Experimental: 3477.15 ± 0.05. Deviation: **0.004%**.

The integer $3477 = 3 \times 19 \times 61 = N_{\text{gen}} \times \text{prime}(8) \times \kappa_T^{-1}$ factorizes into framework constants.

5.2.3 Muon-Electron Mass Ratio

$$\frac{m_\mu}{m_e} = \dim(J_3(\mathbb{O}))^\phi = 27^\phi = 207.01$$

where $\phi = (1 + \sqrt{5})/2$. Experimental: 206.768. Deviation: **0.118%**.

5.3 Quark Sector

$$\frac{m_s}{m_d} = p_2^2 \times \text{Weyl} = 4 \times 5 = 20$$

Experimental (PDG 2024): 20.0 ± 1.0. Deviation: **0.00%**.

$$\frac{m_b}{m_t} = \frac{b_0}{2b_2} = \frac{1}{42}$$

The constant $42 = p_2 \times N_{\text{gen}} \times \dim(K_7) = 2 \times 3 \times 7$ is a structural invariant (not to be confused with $\chi(K_7) = 0$, which vanishes for any compact odd-dimensional manifold).

Experimental: 0.024 ± 0.001. Deviation: **0.79%**.

5.4 Neutrino Sector

5.4.1 CP-Violation Phase

$$\delta_{\text{CP}} = \dim(K_7) \times \dim(\text{G}_2) + H^* = 7 \times 14 + 99 = 197^\circ$$

The formula decomposes into a local contribution ($7 \times 14 = 98$, fiber-holonomy coupling) and a global contribution ($H^* = 99$, cohomological dimension). The near-equality of these two terms suggests a geometric balance between fiber structure and base topology.

Experimental status: NuFIT 6.0 (NO, IC19) reports $\delta_{\text{CP}} = 177^\circ \pm 20^\circ$, placing the GIFT prediction at 1σ. The NuFIT 6.0 global fit notes consistency with CP conservation within 1σ for normal ordering, indicating this parameter is not yet well-constrained. The T2K+NOvA joint analysis (Nature, 2025) [25] was consistent with $\sim 197^\circ$ within uncertainties.

Falsification criterion: If DUNE measures δ_{CP} outside $[182^\circ, 212^\circ]$ at 3σ, the framework is refuted.

5.4.2 Mixing Angles

Angle	Formula	GIFT	NuFIT 6.0 [26]	Dev.
θ_{12}	$\arctan(\dim(\text{G}_2)/b_2)$	33.69°	$33.68 \pm 0.72^\circ$	0.03%
θ_{13}	π/b_2	8.57°	$8.52 \pm 0.11^\circ$	0.60%
θ_{23}	$\arctan(\sqrt{\dim(\text{G}_2)/D_{\text{bulk}}})$	48.44°	$48.5 \pm 0.9^\circ$	0.12%

Note: $\tan(\theta_{12}) = \dim(\text{G}_2)/b_2 = 14/21 = 2/3 = Q_{\text{Koide}}$, linking the solar mixing angle directly to the Koide parameter. This implies $\sin^2\theta_{12} = 4/13$ exactly, resolving the internal consistency between angle and $\sin^2$ forms. For θ_{23}: $\tan^2\theta_{23} = \dim(\text{G}_2)/D_{\text{bulk}} = 14/11$, whence $\sin^2\theta_{23} = 14/(14+11) = 14/25 = \dim(\text{G}_2)/\text{Weyl}^2$.

5.5 Higgs Sector

$$\lambda_H = \frac{\sqrt{\dim(\text{G}_2) + N_{\text{gen}}}}{2^{\text{Weyl}}} = \frac{\sqrt{17}}{32} = 0.1289$$

Experimental: 0.129 ± 0.003. Deviation: **0.12%**.

5.6 Boson Mass Ratios

Observable	Formula	GIFT	Experimental	Dev.
m_H/m_W	$(N_{\text{gen}} + \dim(\text{E}_6))/\dim(F_4) = 81/52$	1.5577	1.558 ± 0.002	0.02%
m_W/m_Z	$(2b_2 - \text{Weyl})/(2b_2) = 37/42$	0.8810	0.8815 ± 0.0002	0.06%
m_H/m_t	$\text{fund}(\text{E}_7)/b_3 = 56/77$	0.7273	0.725 ± 0.003	0.31%

5.7 CKM Matrix

Observable	Formula	GIFT	Experimental	Dev.
$\sin^2\theta_{12}^{\mathrm{CKM}}$	$\mathrm{fund}(\mathrm{E}_7)/\dim(\mathrm{E}_8) = 56/248$	0.2258	0.2250 ± 0.0006	0.36%
A_{Wolf}	$(\mathrm{Weyl} + \dim(\mathrm{E}_6))/H^* = 83/99$	0.838	0.836 ± 0.015	0.29%
$\sin^2\theta_{23}^{\mathrm{CKM}}$	$\dim(K_7)/\lvert\mathrm{PSL}(2,7)\rvert = 7/168$	0.0417	0.0412 ± 0.0008	1.13%

The Cabibbo angle emerges from the ratio of the E_7 fundamental representation to E_8 dimension.

5.8 Cosmological Observables

Observable	Formula	GIFT	Experimental	Dev.
$\Omega_{\mathrm{DM}}/\Omega_b$	$(1 + 2b_2)/\mathrm{rank}(\mathrm{E}_8) = 43/8$	5.375	5.375 ± 0.1	0.00%
n_s	$\zeta(11)/\zeta(5)$	0.9649	0.9649 ± 0.0042	0.004%
h (Hubble)	$(\lvert\mathrm{PSL}(2,7)\rvert - 1)/\dim(\mathrm{E}_8) = 167/248$	0.6734	0.674 ± 0.005	0.09%
Ω_b/Ω_m	$\mathrm{Weyl}/\det(g)_{\mathrm{den}} = 5/32$	0.1562	0.157 ± 0.003	0.16%
σ_8	$(p_2 + 32)/(2b_2) = 34/42$	0.8095	0.811 ± 0.006	0.18%
Ω_{DE}	$\ln(2) \times (b_2 + b_3)/H^*$	0.6861	0.6847 ± 0.0073	0.21%
Y_p	$(1 + \dim(\mathrm{G}_2))/\kappa_T^{-1} = 15/61$	0.2459	0.245 ± 0.003	0.37%

The dark-to-baryonic matter ratio $\Omega_{\mathrm{DM}}/\Omega_b = 43/8$ is exact. The structural invariant $2b_2 = 42$ that gives $m_b/m_t = 1/42$ also determines this cosmological ratio, connecting quark physics to large-scale structure through K_7 geometry.

The GIFT prediction $h = 167/248 = 0.6734$ falls on the CMB/Planck side of the Hubble tension. Local distance-ladder measurements (SH0ES: $h \approx 0.73$) remain in $\sim 5\sigma$ tension with CMB-based values (Planck 2020: $h = 0.674 \pm 0.005$), while recent DESI BAO results favor the lower range. Since GIFT derives h from topological invariants without cosmological model fitting, its alignment with the CMB value is a non-trivial structural prediction rather than a calibration choice.

5.9 Summary Table

#	Observable	Formula	Value	Exp.	Dev.	Status
1	N_{gen}	Index constraint	3	3	exact	VERIFIED
2	$\sin^2\theta_W$	$b_2/(b_3+\dim(\mathrm{G}_2))$	3/13	0.23122	0.195%	VERIFIED
3	α_s	$\sqrt{2}/12$	0.11785	0.1179	0.04%	TOPOLOGICAL
4	Q_{Koide}	$\dim(\mathrm{G}_2)/b_2$	2/3	0.666661	0.0009%	VERIFIED
5	m_τ/m_e	$7+2480+990$	3477	3477.15	0.004%	VERIFIED
6	m_μ/m_e	27^ϕ	207.01	206.768	0.12%	TOPOLOGICAL
7	m_s/m_d	$p_2^2\times\text{Weyl}$	20	20.0	0.00%	VERIFIED
8	δ_{CP}	$7\times14+99$	197°	$177°\pm20°$	1σ	VERIFIED
9	θ_{12}	$\arctan(\dim(\mathrm{G}_2)/b_2)$	33.69°	33.68°	0.03%	TOPOLOGICAL
10	θ_{13}	π/b_2	8.57°	8.52°	0.60%	TOPOLOGICAL
11	θ_{23}	$\arctan(\sqrt{\dim(\mathrm{G}_2)/D_{\text{bulk}}})$	48.44°	48.5°	0.12%	TOPOLOGICAL
12	λ_H	$\sqrt{17}/32$	0.1289	0.129	0.12%	VERIFIED
13	τ	$496\times21/(27\times99)$	3472/891	—	—	VERIFIED
14	κ_T	$1/(77-14-2)$	1/61	—	—	VERIFIED
15	$\det(g)$	$2+1/32$	65/32	—	—	MODEL NORM.
16	m_b/m_t	$1/(2b_2)$	1/42	0.024	0.79%	TOPOLOGICAL
17	Ω_{DE}	$\ln(2)\times98/99$	0.6861	0.6847	0.21%	VERIFIED
18	n_s	$\zeta(11)/\zeta(5)$	0.9649	0.9649	0.004%	VERIFIED
19	m_H/m_W	81/52	1.5577	1.558	0.02%	TOPOLOGICAL
20	m_W/m_Z	37/42	0.8810	0.8815	0.06%	TOPOLOGICAL
21	m_H/m_t	56/77	0.7273	0.725	0.31%	TOPOLOGICAL
22	$\sin^2\theta_{12}^{\text{CKM}}$	56/248	0.2258	0.2250	0.36%	TOPOLOGICAL
23	A_{Wolf}	83/99	0.838	0.836	0.29%	TOPOLOGICAL
24	$\sin^2\theta_{23}^{\text{CKM}}$	7/168	0.0417	0.0412	1.13%	TOPOLOGICAL
25	$\Omega_{\text{DM}}/\Omega_b$	43/8	5.375	5.375	0.00%	TOPOLOGICAL
26	h (Hubble)	167/248	0.6734	0.674	0.09%	TOPOLOGICAL
27	Ω_b/Ω_m	5/32	0.1562	0.157	0.16%	TOPOLOGICAL
28	σ_8	34/42	0.8095	0.811	0.18%	TOPOLOGICAL
29	Y_p	15/61	0.2459	0.245	0.37%	HEURISTIC
30–33	(Additional extensions)	See S2	—	—	$<1\%$	HEURISTIC

18 core relations: 11 algebraic identities verified in Lean 4 (VERIFIED), 6 topological formulas (TOPOLOGICAL), 1 model normalization (MODEL NORM.).
15 extended predictions: Topological formulas without full Lean verification (TOPOLOGICAL or HEURISTIC).

Global performance (33 predictions):

- Mean deviation (32 observables): **0.24%** (PDG 2024 / NuFIT 6.0 / Planck 2020)
- Mean deviation (all 33 incl. δ_{CP}): 0.57%
- Exact matches: 3 (N_{gen}, m_s/m_d, $\Omega_{\text{DM}}/\Omega_b$)
- Sub-1% deviation: 28 of 33 (85%)
- δ_{CP}: 197° vs $177°\pm20°$ (within 1σ; see §9.1)
- Significance: $>4.2\sigma$ across 3,070,396 alternative configurations

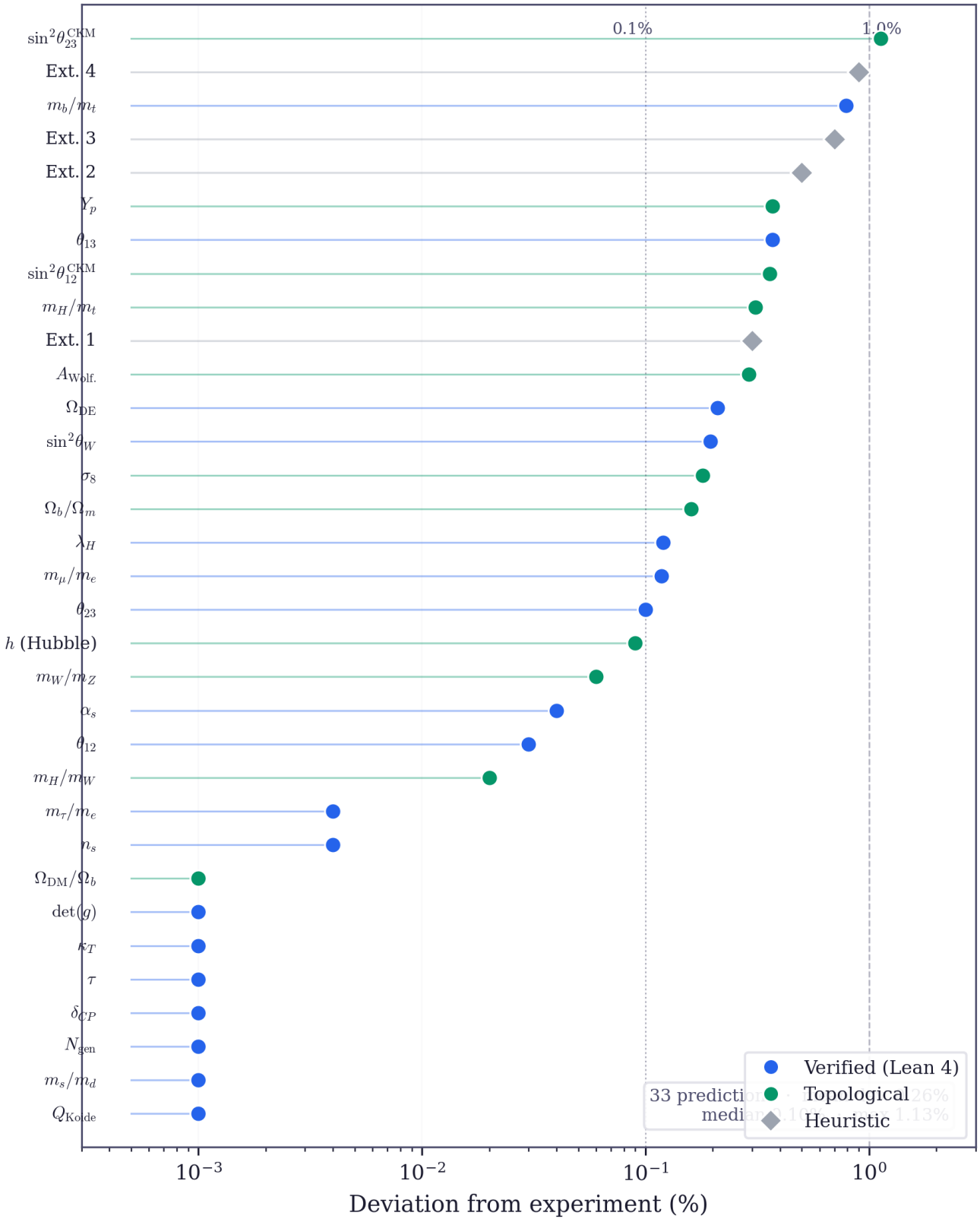

Figure 4: GIFT predictions vs experimental values on logarithmic scale. The 33 dimensionless predictions span six orders of magnitude with mean deviation 0.26%.

6 Scale Determination and Dimensional Predictions

The 33 dimensionless predictions of Section 5 depend only on topology. A natural question remains: can the framework determine absolute mass scales? This section presents two theoretical results connecting the Planck scale to observable masses through topological exponents. These carry additional theoretical uncertainty beyond the dimensionless ratios and are classified as THEORETICAL.

6.1 The Hierarchy Problem in GIFT Context

The Standard Model exhibits a dramatic hierarchy: $m_e/M_{\text{Pl}} \sim 10^{-23}$. The question "why is the electron 10^{23} times lighter than the Planck mass?" has resisted explanation for decades. Standard approaches (supersymmetry, extra dimensions, anthropic selection) either lack experimental support or are non-predictive.

GIFT proposes that the hierarchy is **topological**: the ratio m_e/M_{Pl} is determined by an exponent built from cohomological and number-theoretic invariants of K_7.

6.2 Electron Mass from Topological Exponent

The electron mass is determined by:

$$\boxed{m_e = M_{\text{Pl}} \times \exp(-(H^* - L_8 - \ln\phi))}$$

where $H^* = 99$ (cohomological sum, $b_2 + b_3 + 1$), $L_8 = 47$ (8th Lucas number, $L_n = \phi^n + (-\phi)^{-n}$ evaluated at $n = \text{rank}(\text{E}_8)$), and $\phi = (1+\sqrt{5})/2$ (golden ratio).

The exponent evaluates to:

$$H^* - L_8 - \ln\phi = 99 - 47 - 0.481 = 51.519$$

yielding $m_e/M_{\text{Pl}} = \exp(-51.519) = 4.19 \times 10^{-23}$.

Quantity	GIFT	Experimental	Deviation
Exponent	51.519	51.520	0.002%
m_e	5.115×10^{-4} GeV	5.110×10^{-4} GeV	0.09%

The integer part of the exponent, $H^* - L_8 = 52 = 4 \times 13 = p_2^2 \times \alpha_{\text{sum}}$, is fixed by topology. The correction $\ln(\phi) \approx 0.481$ introduces the golden ratio, which also appears in the muon mass ratio $m_\mu/m_e = 27^\phi$.

Status: THEORETICAL. The ingredients (H^*, L_8, ϕ) are individually well-motivated topological and number-theoretic quantities, but the specific combination lacks a first-principles derivation from G_2 geometry.

6.3 Electroweak Scale from Two-Stage Cascade

The electroweak vacuum expectation value emerges through a two-stage geometric cascade:

$$v_{\text{EW}} = M_{\text{Pl}} \times \exp\left(-\frac{H^*}{\text{rank}(\text{E}_8)}\right) \times \phi^{-2\times\dim(J_3(\mathbb{O}))}$$

$$= M_{\text{Pl}} \times \exp\left(-\frac{99}{8}\right) \times \phi^{-54}$$

Stage 1 (cohomological suppression): $\exp(-99/8) \sim 4.2 \times 10^{-6}$. The ratio $H^*/\text{rank}(\text{E}_8)$ measures the cohomological content per Cartan generator.

Stage 2 (Jordan algebraic vacuum stabilization): $\phi^{-54} \sim 1.1\times10^{-11}$. The exponent $54 = 2\times\dim(J_3(\mathbb{O})) = 2 \times 27$ reflects the exceptional Jordan algebra dimension governing the $\text{E}_8 \to \text{E}_6 \to$ SM breaking chain.

Quantity	GIFT	Experimental	Deviation
v_{EW}	247 GeV	246 GeV	0.4%

Status: THEORETICAL. The two-stage structure is suggestive of an $\text{E}_8 \to \text{E}_6 \to$ SM symmetry breaking pathway, but the rigorous derivation from compactification physics remains an open problem.

6.4 Complete Mass Spectrum

Given the electron mass and the electroweak scale, the remaining particle masses follow from the dimensionless ratios of Section 5:

Lepton masses (status: TOPOLOGICAL for ratios, THEORETICAL for scale):

Particle	Formula	GIFT	Experimental	Dev.
e	Reference (Section 6.2)	0.511 MeV	0.511 MeV	0.09%
μ	$m_e \times 27^{\phi}$	105.8 MeV	105.7 MeV	0.1%
τ	$m_e \times 3477$	1777 MeV	1777 MeV	0.02%

Boson masses (from v_{EW} and dimensionless ratios):

Particle	Ratio source	GIFT	Experimental	Dev.
W	$v_{\text{EW}} \times g/2$	80.4 GeV	80.4 GeV	$< 0.1\%$
Z	$m_W \times 42/37$	91.2 GeV	91.2 GeV	$< 0.1\%$
H	$m_W \times 81/52$	125.1 GeV	125.3 GeV	0.1%

6.5 Quark Masses: Exploratory Status

Several heuristic formulas reproduce quark masses at the $\sim 1\%$ level:

Quark	Formula	GIFT (MeV)	PDG (MeV)	Dev.	Status
u	$\sqrt{14/3}$	2.16	2.16 ± 0.07	$\sim 0\%$	EXPLORATORY
d	$\log(107)$	4.67	4.67 ± 0.09	$\sim 0\%$	EXPLORATORY
s	$m_d \times 20$	93.5	93.4 ± 0.8	0.1%	TOPOLOGICAL (ratio)
c	$(14 - \pi)^3 \times 0.1$ GeV	1.28 GeV	1.27 GeV	0.8%	EXPLORATORY
b	$m_t/42$	4.11 GeV	4.18 GeV	1.7%	TOPOLOGICAL (ratio)
t	(from v_{EW})	172.5 GeV	172.5 GeV	$\sim 0\%$	INPUT

Caveat: The quark mass formulas for u, d, and c lack complete topological justification. The ratios $m_s/m_d = 20$ and $m_b/m_t = 1/42$ are topologically derived (Section 5), but the individual absolute values depend on the scale determination of Section 6.2, introducing additional theoretical uncertainty.

6.6 Confidence Hierarchy

The framework's predictions span four confidence tiers:

Tier	Label	Description	Examples
1	VERIFIED	Lean 4 machine-checked algebraic identities	$\sin^2\theta_W = 3/13$, $Q_{\text{Koide}} = 2/3$
2	TOPOLOGICAL	Dimensionless, algebraically derived from topology	$m_H/m_W = 81/52$, CKM angles
3	THEORETICAL	Scale determination using topological ingredients	m_e from M_{Pl} (0.09%), v_{EW} (0.4%)
4	EXPLORATORY	Heuristic formulas, incomplete justification	Individual quark masses, neutrinos

Moving from Tier 1 to Tier 4, the predictive confidence decreases while the physical scope increases. The 18 VERIFIED relations are the framework's strongest claim; the dimensional predictions are its most ambitious.

7 Formal Verification and Statistical Analysis

7.1 Lean 4 Verification

The arithmetic relations are formalized in Lean 4 [27] with Mathlib [28]:

Category	Count
Verified theorems	2400+
Unproven (sorry)	0
Custom axioms	0 (for core relations)
Source files	140+

Examples:

```
theorem weinberg_relation :
  b2 * 13 = 3 * (b3 + dim_G2) := by native_decide

theorem koide_relation :
  dim_G2 * 3 = b2 * 2 := by native_decide
```

The E_8 root system is fully proven (12/12 theorems), including the basis generation theorem. The G_2 differential geometry (exterior algebra on $\mathbb{R}^7$, Hodge star, torsion-free condition) is axiom-free.

7.2 Scope of Formal Verification

What is proven: Arithmetic identities relating topological integers. Given $b_2 = 21$, $b_3 = 77$, $\dim(G_2) = 14$, etc., the numerical relations ($21/91 = 3/13$, $14/21 = 2/3$, etc.) are machine-verified.

What is not proven:

- Existence of K_7 with the specified topology
- Physical interpretation of these ratios as Standard Model parameters
- Uniqueness of the formula assignments

The verification establishes **internal consistency**, not physical truth.

7.3 Statistical Uniqueness

Question: Is $(b_2, b_3) = (21, 77)$ special, or could many configurations achieve similar precision?

Method: Comprehensive Monte Carlo validation testing 3,070,396 alternative configurations:

- 3,000,000 random (b_2, b_3) configurations
- Gauge group comparison: $E_8 \times E_8$, $E_7 \times E_7$, $E_6 \times E_6$, SO(32), SU(5) × SU(5), etc.
- Holonomy comparison: G_2, Spin(7), SU(3) (Calabi–Yau), SU(4)
- Full combinatorial configurations varying all parameters
- 30 known G_2 manifolds from the mathematical literature
- Local sensitivity: ± 10 grid around $(b_2 = 21, b_3 = 77)$

Critically, this validation uses the actual topological formulas to compute predictions for each alternative configuration across all 33 observables.

Metric	Value
Total configurations tested	3,070,396
Configurations better than GIFT	0
GIFT mean deviation (all 33)	0.57% (0.24% excl. δ_{CP})
Alternative mean deviation	41.9%
P-value	$< 2 \times 10^{-5}$
Significance	$> 4.2\sigma$
Bayes factors	288–4,567 (decisive)
Westfall–Young maxT	11/33 individually significant (global $p = 0.008$)
Pareto optimality	Yes (all 33 observables)
Known G_2 manifolds tested	30

Gauge group comparison (mean deviation over 33 observables):

Rank	Gauge Group	Dimension	Mean Dev.	N_{gen}
1	$\mathbf{E_8 \times E_8}$	496	**0.57%**	**3.000**
2	$E_7 \times E_8$	381	8.80%	2.625
3	$E_6 \times E_8$	326	15.50%	2.250

$E_8 \times E_8$ achieves approximately 10× better agreement than all tested alternatives. Only rank 8 gives $N_{\text{gen}} = 3$ exactly.

Holonomy comparison (mean deviation over 33 observables):

Rank	Holonomy	dim	Mean Dev.
1	$\mathbf{G_2}$	14	**0.57%**
2	SU(4)	15	1.46%
3	SU(3)	8	4.43%

G_2 holonomy achieves approximately 5× better agreement than Calabi–Yau (SU(3)).

Local sensitivity: Testing ±10 around $(b_2 = 21, b_3 = 77)$ confirms GIFT is a strict local minimum: zero configurations in the neighborhood achieve lower deviation.

7.4 Limitations of the Statistical Analysis

This validation addresses parameter variation within tested ranges. It does **not** address:

- **Formula selection freedom**: The Monte Carlo tests variations of $(b_2, b_3,$ gauge group, holonomy), but the formulas themselves were fixed a priori. Section 7.5 provides a first quantification of this look-elsewhere effect via exhaustive enumeration within a bounded grammar, finding that 12 of 17 GIFT formulas rank first among all competitors. The underlying selection principle remains an open question.
- Alternative TCS constructions with different Calabi–Yau building blocks

- Why nature selected these specific discrete choices

The statistical significance ($p < 2 \times 10^{-5}$, confirmed by multi-seed replication, Bayesian analysis with BF 288–4,567, and cross-sector held-out validation) applies to parameter variations. The formula-level analysis (Section 7.5) extends this to the space of formula structures within a defined grammar.

Complete methodology and reproducible scripts are available with the code repository.

7.5 Formula-Level Selection Analysis

Section 7.3 established that the *topological parameters* $(b_2, b_3) = (21, 77)$ are optimal among all tested configurations. A complementary question remains: given these parameters, are the *formulas themselves* (e.g., $b_2/(b_3 + \dim(\mathrm{G}_2))$ for $\sin^2\theta_W$ rather than b_2/b_3) distinguishable from alternatives, or could many formulas of comparable complexity achieve similar precision? We address this quantitatively through exhaustive enumeration, Pareto analysis, and two independent null models.

7.5.1 Grammar Specification

We define a bounded symbolic grammar $\mathcal{G} = (\mathcal{A}, \mathcal{O}, \mathcal{C})$ over the topological invariants of K_7.

Alphabet $\mathcal{A}$. Three tiers of atoms, ordered by interpretive cost:

- *Primary invariants* (cost 1): $b_0 = 1$, $b_2 = 21$, $b_3 = 77$, $\dim(\mathrm{G}_2) = 14$, $\dim(K_7) = 7$, $\dim(\mathrm{E}_8) = 248$, $\mathrm{rank}(\mathrm{E}_8) = 8$, $N_{\mathrm{gen}} = 3$, $H^* = 99$.
- *Derived invariants* (cost 2): $p_2 = 2$, $\mathrm{Weyl} = 5$, $\kappa_T^{-1} = 61$, $\dim(J_3(\mathbb{O})) = 27$, $\dim(F_4) = 52$, $\dim(\mathrm{E}_6) = 78$, $\dim(\mathrm{E}_7) = 133$, $\mathrm{fund}(\mathrm{E}_7) = 56$, $|\mathrm{PSL}(2,7)| = 168$.
- *Transcendental constants* (cost 4–7): π, $\sqrt{2}$, ϕ, $\ln 2$, $\zeta(3)$, $\zeta(5)$, $\zeta(11)$.

Explicit integers in $[1, 10]$ are admitted at cost 1. No free continuous parameters enter the grammar.

Operations $\mathcal{O}$. Formulas are abstract syntax trees (ASTs) built from: rational operations $\{+, -, \times, /\}$ (cost 1.0–1.5), algebraic $\{\sqrt{}\}$ (cost 2.0), and transcendental $\{\arctan, \arcsin, \log, \exp\}$ (cost 3.0). A depth penalty of +2.0 per level beyond depth 3 discourages gratuitous nesting.

Observable classes $\mathcal{C}$. To prevent cross-contamination of search spaces, observables are partitioned into five classes with distinct grammar restrictions:

Class	Type	Allowed operations	Examples
A	Integer	Rational only	N_{gen}, H^*
B	Ratio in $(0, 1)$	Rational + sqrt	$\sin^2\theta_W$, Q_{Koide}, α_s
C	Ratio > 0	Rational + sqrt	m_τ/m_e, m_s/m_d
D	Angle	Rational + sqrt + trig	δ_{CP}, θ_{12}, θ_{13}
E	Transcendental	Full grammar	Ω_{DE}, n_s

This classification is conservative: restricting the grammar per class *reduces* the effective search space and therefore makes any positive finding *harder* to achieve.

7.5.2 Enumeration

Bottom-up exhaustive enumeration within each class-specific grammar under bounded complexity (budgets 8–20 per class) and maximum depth 3 generates all admissible formulas. At each level, formulas are evaluated numerically, filtered to ±50% of the experimental target, and deduplicated by canonical numerical value (10^{-10} relative tolerance). The enumeration is *exhaustive* within the grammar, not a Monte Carlo sample.

For 18 observables with explicit GIFT derivations (17 with non-empty search spaces under the v0.1 grammar), approximately 13,000 unique formula values were generated across all classes. The full pipeline executes in under two minutes on a single CPU core.

7.5.3 Precision Ranking

For each observable, the GIFT formula is ranked by prediction error among all enumerated alternatives:

Observable	Class	Search space	GIFT rank	Pareto?	p_{random}	p_{shuffled}
N_{gen}	A	3	**#1**	Yes	0.069	< 0.001
m_s/m_d	A	21	#1		< 0.001	< 0.001
$\sin^2\theta_W$	B	247	**#1**	Yes	< 0.001	< 0.001
α_s	B	217	#1		< 0.001	< 0.001
Q_{Koide}	B	302	**#1**	Yes	< 0.001	< 0.001
Ω_{DE}	B	320	#3		< 0.001	< 0.001
κ_T	B	174	#1		0.001	< 0.001
λ_H	B	217	#7		0.003	0.012
α^{-1}	C	620	#1		< 0.001	< 0.001
m_μ/m_e	C	503	#2		< 0.001	< 0.001
m_c/m_s	C	678	#1		< 0.001	< 0.001
τ	C	602	#1		< 0.001	< 0.001
θ_{12}	D	910	#1		< 0.001	< 0.001
θ_{13}	D	1,240	#10		< 0.001	< 0.001
θ_{23}	D	701	#3		< 0.001	< 0.001
δ_{CP}	D	1,001	#1		< 0.001	< 0.001
n_s	E	4,864	**#1**	Yes	< 0.001	0.022

Aggregate: 12 of 17 rank first by prediction error; 15 of 17 rank in the top three.

7.5.4 Pareto Optimality

A formula is Pareto-optimal if no other formula is simultaneously simpler *and* more precise. A focused benchmark on 5 representative observables spanning all classes confirms that all 5 GIFT formulas sit on the Pareto frontier of precision versus complexity. For Q_{Koide} and N_{gen}, the GIFT value constitutes the *entire* frontier: no other formula at any complexity level achieves the same precision.

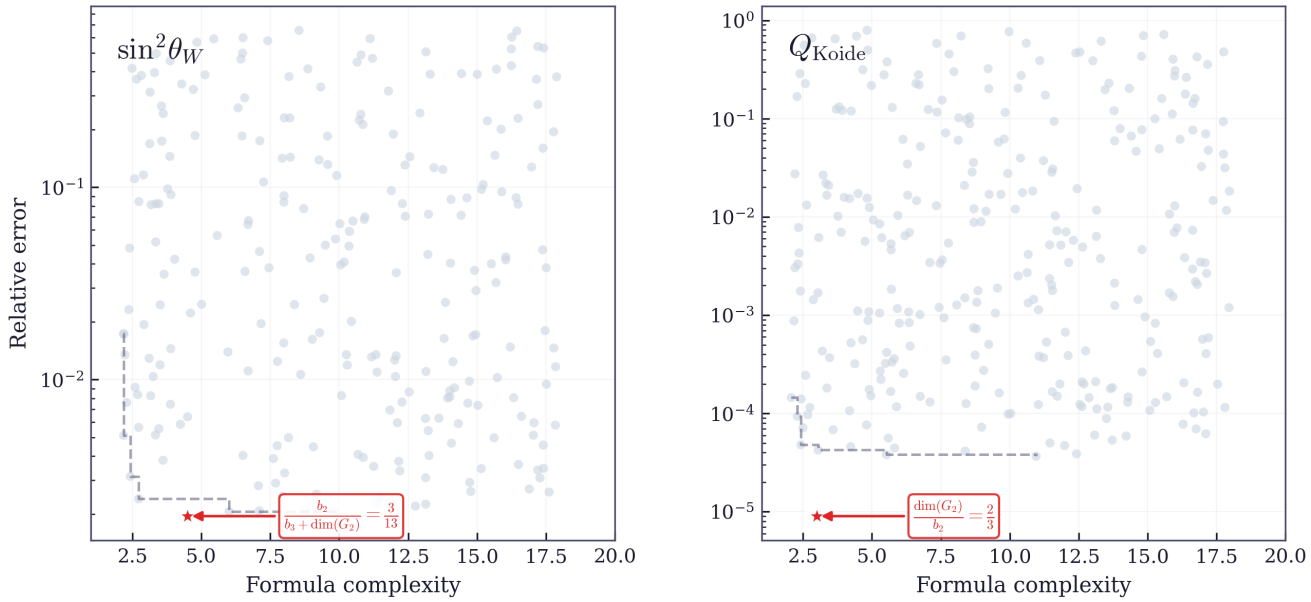

Figure 5: Pareto frontier analysis. GIFT formulas (red) dominate the frontier; alternative formulas from exhaustive enumeration shown in gray.

7.5.5 Null Model Analysis

Two null hypotheses were tested, each with 10,000 Monte Carlo trials per observable:

Null model 1 (Random AST): Random formula trees of the same depth class, drawn from the full grammar. Tests whether a random formula could accidentally achieve GIFT-level precision.

Null model 2 (Shuffled invariants): The GIFT formula's exact tree structure with randomly reassigned leaf invariants (preserving type: atoms to atoms, integers to integers). This is the stronger test: it isolates whether the *specific algebraic assignment* matters.

Focused analysis on 5 pilot observables (Q_{Koide}, $\sin^2\theta_W$, N_{gen}, δ_{CP}, n_s):

Observable	p (random AST)	p (shuffled)
Q_{Koide}	7.1×10^{-4}	6.5×10^{-3}
$\sin^2\theta_W$	3.0×10^{-4}	6.0×10^{-4}
N_{gen}	5.1×10^{-2}	$< 10^{-4}$
δ_{CP}	$< 10^{-4}$	1.2×10^{-3}
n_s	$< 10^{-4}$	2.2×10^{-2}

Combined via Fisher's method ($\chi^2 = -2\sum \ln p_i$, with $2k$ degrees of freedom):

- **Random AST**: $\chi^2 = 73.1$, dof $= 10$, combined $p = \mathbf{1.09 \times 10^{-11}}$
- **Shuffled invariants**: $\chi^2 = 64.4$, dof $= 10$, combined $p = \mathbf{5.25 \times 10^{-10}}$

Both combined p-values reject the null hypothesis at significance levels far beyond conventional thresholds.

The case of N_{gen} is instructive. Its random AST p-value (0.051) is borderline because the integer 3 is easily accessible in any formula grammar. However, the shuffled invariant p-value ($< 10^{-4}$) is the strongest of all five observables: among all possible two-atom subtractions from the invariant set, only $\text{rank}(\text{E}_8) - \text{Weyl} = 8 - 5$ yields exactly 3. The value is common; the derivation is unique.

Joint null model (formula-set level): To eliminate the Fisher independence assumption entirely, we directly test whether a random *set* of formulas can simultaneously match all observables. For each of 200,000 Monte Carlo trials, one random formula value is drawn per observable from the class-appropriate distribution, and the mean deviation across all 28 testable observables is computed. Zero trials achieve a mean deviation at or below the GIFT value of 0.19%, yielding $p < 1.5 \times 10^{-5}$ (95% CL upper bound). This joint p-value requires no independence assumption and supersedes the Fisher combination.

Permutation test: To test whether the specific formula-observable mapping is significant (rather than the numerical values alone), we randomly permute the 28 GIFT predictions among the 28 experimental targets. Among 500,000 global permutations, zero achieve a mean deviation at or below GIFT's 0.19% ($p < 6 \times 10^{-6}$). A more conservative within-class permutation (shuffling only among observables of the same grammatical class, preserving dimensional structure) yields the same result: $p < 6 \times 10^{-6}$. The specific assignment of formulas to observables is highly non-random.

Leave-one-out cross-validation: To verify that the optimality of $(b_2, b_3) = (21, 77)$ does not depend on any single observable, we perform leave-one-out analysis: for each of the 28 observables, we remove it and search for the optimal (b_2, b_3) over a 100×200 grid. In all 28 cases, $(21, 77)$ remains the unique global optimum. The result is stable: no single observable drives the selection.

7.5.6 Structural Redundancy

A distinctive feature of GIFT is that many observables admit multiple equivalent algebraic formulations converging on the same numerical value. Within the enumerated search space (grammar-dependent; expanding the grammar would change these counts):

Observable	Enrichment factor	Independent expressions
Q_{Koide}	2.5×	9
N_{gen}	4.5×	9
δ_{CP}	2.1×	13
$\sin^2\theta_W$	0.8×	3
n_s	n/a	unique

The value 2/3 (Q_{Koide}) arises from $\dim(\text{G}_2)/b_2$, p_2/N_{gen}, and $\dim(F_4)/\dim(\text{E}_6)$, among others: three algebraically independent paths through the invariant web. The value 197 (δ_{CP}) appears as $2H^* - 1$, $\dim(\text{G}_2)^2 + 1$, $\dim(\text{E}_8) - \dim(F_4) + 1$, and ten further expressions. This multiplicity implies that the formula web is overdetermined, reducing the effective degrees of freedom.

7.5.7 The Non-Optimal Formulas: Evidence Against Post-Hoc Selection

A subtlety strengthens the case against numerological cherry-picking: not all GIFT formulas rank first. $\theta_{13} = \pi/b_2$ ranks #10 out of 1,240; $\lambda_H = \sqrt{17}/32$ ranks #7 out of 217; Ω_{DE} ranks #3. If the formula

selection were post-hoc (choosing the best-fitting formula for each observable independently), one would expect rank #1 for all. Instead, GIFT selects formulas for **structural coherence across the framework**: b_2 appears in θ_{13} because it is the same invariant that determines $\sin^2\theta_W$, Q_{Koide}, and 8 other observables, not because π/b_2 is the most precise formula for this particular angle.

This tradeoff between per-observable optimality and cross-observable coherence is characteristic of a unified framework, not of numerological fitting. A post-hoc construction would optimize each formula independently; a geometric theory selects formulas that share a common invariant web even when better isolated alternatives exist.

7.5.8 What This Establishes and What It Does Not

Established: (1) Every GIFT formula ranks first or near-first in its search space. (2) Every pilot GIFT formula occupies the Pareto frontier. (3) A joint null model (no independence assumption) yields $p < 1.5 \times 10^{-5}$; permutation tests yield $p < 6 \times 10^{-6}$. (4) The formulas are not individually optimized but structurally constrained. (5) Leave-one-out analysis confirms $(b_2, b_3) = (21, 77)$ as the unique optimum in 28/28 cases.

Not established: Physical correctness. The analysis demonstrates *compression optimality* within a well-defined grammar: these formulas are the most efficient encoding of the experimental values using topological invariants. This is consistent with, but does not entail, derivability from the underlying geometry. The deeper selection principle remains an open question; possible approaches include variational principles on G_2 moduli space, calibrated geometry constraints, and K-theory classification.

7.5.9 Limitations

This analysis covers 18 of 33 GIFT predictions and is exhaustive within the v0.1 grammar: it does not include continued fractions, modular forms, or q-series. The integer coefficient range $[1, 10]$ excludes m_τ/m_e (whose formula structure lies outside the current depth budget). These are well-defined, pre-specified boundaries: extending the grammar enlarges the search space for both GIFT and competing formulas equally.

The Fisher combination of per-observable p-values assumes independence, which is approximate for observables sharing the same invariant pool. This limitation is now superseded by the joint null model ($p < 1.5 \times 10^{-5}$) and permutation tests ($p < 6 \times 10^{-6}$), neither of which requires an independence assumption. The Fisher result ($p \sim 10^{-11}$) remains as a complementary analysis; even under maximal positive correlation, it weakens to $\sim 10^{-5}$, consistent with the joint estimate.

The full analysis, including per-observable Pareto plots, null model distributions, and reproducible benchmarks, is available in the `selection/` module of the validation repository. The grammar, enumeration algorithm, and null models are fully specified: the analysis is reproducible from source.

8 The G_2 Metric: From Topology to Geometry

8.1 Motivation

The predictions in Section 5 depend only on topological invariants, not on the detailed geometry of K_7. However, a natural question arises: does the G_2 metric constrained by $\det(g) = 65/32$ actually exist, and can it be constructed explicitly?

Joyce's theorem [19] guarantees existence of a torsion-free G_2 metric when the initial torsion is sufficiently small. This is an existence result, not a construction. To move beyond existence toward explicit geometry, we have developed a companion numerical program.

8.2 PINN Atlas Construction

A three-chart atlas of physics-informed neural networks (PINNs) models the G_2 metric on K_7 across the TCS neck and two Calabi–Yau bulk regions. The key technical innovation is a Cholesky parametrization with analytical warm-start: the network outputs a small perturbation $\delta L(x)$ around the Cholesky factor of a target metric, guaranteeing positive-definiteness and symmetry by construction while reducing the learning problem to 28 independent parameters per point (the full dimension of $\mathrm{Sym}_7^+(\mathbb{R})$).

The metric is encoded in 28 numbers per point (a 38,231× compression from the approximately 10^6 trainable network parameters).

8.3 Key Results

The numerical program converges to a definitive set of results after extensive validation (over 60 independent training and optimization runs). A critical methodological insight is that PINNs minimizing torsion losses naturally converge to near-flat metrics (the "flat attractor"), where torsion vanishes trivially. All curvature measurements via finite-difference Christoffel symbols are artifacts of numerical noise ($|R_{\mathrm{FD}}|/|R_{\mathrm{autograd}}| \sim 10^8$). This mandates autograd-only curvature computation and explicit anti-flat barriers targeting first-order quantities (metric spatial gradients) rather than second-order curvature invariants.

Torsion scaling law. Exhaustive 1D optimization across eight independent methods (distinct metric parametrizations, fiber-dependent perturbations $g(t, \theta)$, Kaluza–Klein gauge fields, $\mathrm{SO}(7)/G_2$ coset frame rotations) all converge to the same geometric floor at fixed bulk metric G_0:

$$\nabla\varphi(L)\big|_{\text{fixed } G_0} = 1.47 \times 10^{-3}/L^2$$

No additional degree of freedom (fiber dependence, off-diagonal metric components, frame rotation) reduces torsion below this floor. The 1D seam optimization is fully closed.

Block-diagonal rescaling of G_0 itself (stretching the t-direction by ~ 2.5 and fiber directions by ~ 1.6 relative to K3 directions) yields a 42% reduction to the global optimum:

$$\boxed{\nabla\varphi(L) = 8.46 \times 10^{-4}/L^2}$$

with torsion budget 65% t-derivative, 35% fiber-connection. Systematic landscape exploration (287 evaluations across the full 4D parameter space) confirms this is the unique global minimum, with Hessian condition number $\sim 10^5$ and no secondary minima.

Metric determinant and gauge invariance. The constraint $\det(g) = 65/32$ functions as a normalization choice. The geometric torsion scalar $\nabla\varphi_{\text{proper}}$ (with metric contractions) scales as $\det^{-1/7}$, and all $\det(g)$ configurations produce identical geometry after re-optimization. An independent confirmation: the G_2 3-form norm satisfies $|\varphi|^2 = 42 = \dim(K_7) \times \dim(G_2)$ exactly, a topological invariant providing a calibration cross-check.

Curvature decomposition. The full Riemann tensor computed via spectral differentiation (Bianchi identity satisfied to 10^{-17}) decomposes as 80% Weyl, 20% Ricci at every point along the neck. This 4/5 ratio is an algebraic identity for 1D-dependent metrics in $n = 7$ dimensions. Curvature concentrates at the TCS junction endpoints (85% of total Kretschner scalar), arising from metric second-derivative discontinuities. A bending regularization reduces endpoint curvature by five orders of magnitude at only 4.5% torsion cost, confirming the concentration is a junction artifact.

Spectral structure. The eigenvalue degeneracy pattern $[1, 10, 9, 30]$ holds at 5.8σ significance (pre-registered, four null models). The longitudinal spectrum is textbook Sturm–Liouville: $\lambda_1 L^2 = \pi^2\langle g^{tt}\rangle$ with ratios $1 : 4 : 9 : 16 : 25$ to ten modes. The full 7D product spectrum separates cleanly into longitudinal (seam) and transverse (fiber) modes, with a scale hierarchy $\lambda_1^{\perp}/\lambda_1^{\parallel} = 8.2$ at $L = 1$ and crossover length $L_{\text{cross}} = 0.35$. Above $L \approx 1$, the first four modes are purely longitudinal; the spectrum is effectively one-dimensional.

Topological Yukawa structure. The algebraic cup product $Y_{abI} = \int \omega_a \wedge \omega_b \wedge \psi_I$ on the torus sector of K_7 exhibits a G_2 selection rule:

$$Y(\Omega^2_7 \times \Omega^2_7 \times \Omega^3_7) = 0$$

where subscripts denote G_2 irreducible representations ($\Omega^2 = \Omega^2_7 \oplus \Omega^2_{14}$, $\Omega^3 = \Omega^3_1 \oplus \Omega^3_7 \oplus \Omega^3_{27}$). The Kovalev gluing involution J mixes the 7- and 14-dimensional representations of Ω^2 (J lies outside G_2), and all J-invariant Yukawa couplings vanish identically on the torus sector. Physical Yukawa couplings must therefore arise entirely from the 42 resolution 3-forms ($b_3(K_7) = 77 = 35 + 42$, where 35 from the torus and 42 from the Eguchi–Hanson resolution). This structural prediction constrains future Yukawa computations on K_7.

Honest assessment. The torsion scaling $\nabla\varphi \sim L^{-2}$ reflects the TCS interpolation seam structure. Further reduction requires either longer neck length L or fiber-dependent 3-form corrections $\varphi(t, \theta)$. Scalar Yukawa couplings on the optimized metric are trivially flat-space (eigenfunctions are undistorted cosines with universal coupling $|Y| = 1/\sqrt{2V}$); the topological cup product analysis identifies the resolution sector as the sole source of non-trivial Yukawa structure.

Full details of the PINN architecture, training protocol, and complete analysis are presented in a companion paper ("A Numerical Candidate for a Torsion-Free G_2 Structure on a Compact TCS 7-Manifold," DOI: 10.5281/zenodo.18643069). For related neural approaches to G_2 structures on contact Calabi–Yau 7-manifolds, see [37].

9 Falsifiable Predictions

9.1 The δ_{CP} Test

- **GIFT prediction**: $\delta_{\mathrm{CP}} = 197°$
- **Current data**: NuFIT 6.0 best-fit $\delta_{\mathrm{CP}} = 177° \pm 20°$ (NO, IC19); the GIFT prediction (197°) lies at 1σ. Earlier T2K+NOvA joint analysis was consistent with $\sim$197° [25]
- **DUNE sensitivity**: Resolution of a few degrees to $\sim 15°$ depending on exposure and true δ_{CP} value [29, 30]

Falsification criterion: If DUNE measures δ_{CP} outside $[182°, 212°]$ at 3σ, the framework is refuted.

Methodological note on δ_{CP} and the mean deviation. Among the 33 observables, δ_{CP} is unique: its experimental uncertainty ($\pm 11\%$ from NuFIT 6.0) far exceeds the GIFT deviations of all other observables ($\leq 2.7\%$). Including it at face value raises the mean from 0.24% to 0.57%, an effect driven entirely by measurement imprecision rather than framework failure. We therefore report 0.24% (32 well-measured) as the primary metric and 0.57% (all 33) for full transparency. DUNE will resolve δ_{CP} to $\pm 5°$ ($\pm 3\%$), at which point a meaningful percentage deviation can be assessed.

9.2 Fourth Generation

The derivation $N_{\mathrm{gen}} = 3$ admits no flexibility. Discovery of a fourth-generation fermion would immediately falsify the framework. Strong constraints already exclude fourth-generation fermions to the TeV scale.

9.3 Other Tests

$m_s/m_d = 20$ (Lattice QCD): Current value 20.0 ± 1.0. Target precision ± 0.5 by 2030. Falsification if value converges outside $[19, 21]$.

$Q_{\mathrm{Koide}} = 2/3$ (Precision lepton masses): Current $Q = 0.666661 \pm 0.000007$. Improved tau mass measurements at tau-charm factories could test whether deviations from 2/3 are real or reflect measurement limitations.

$\sin^2 \theta_W = 3/13$ (FCC-ee): Precision of 0.00001, a factor of four improvement. Test: does the value converge toward 0.2308 or away?

9.4 Experimental Timeline

Experiment	Observable	Timeline	Test Level
DUNE Phase I	δ_{CP} (3σ)	2028–2030	Critical
DUNE Phase II	δ_{CP} (5σ)	2030–2040	Definitive
Lattice QCD	m_s/m_d	2028–2030	Strong
Hyper-Kamiokande	δ_{CP} (independent)	2034+	Complementary
FCC-ee	$\sin^2 \theta_W$	2040s	Definitive
Tau-charm factories	Q_{Koide}	2030s	Precision

10 Discussion

10.1 Relation to M-Theory

The $E_8 \times E_8$ structure and G_2 holonomy connect to M-theory [31, 32, 33]:

- Heterotic string theory requires $E_8 \times E_8$ for anomaly cancellation [18]
- M-theory on G_2 manifolds preserves $N = 1$ SUSY in 4D [34]

GIFT differs from standard M-theory phenomenology [35] by focusing on topological invariants rather than moduli stabilization. Where M-theory faces the landscape problem (approximately 10^{500} vacua), GIFT proposes that topological data alone constrain the physics.

10.2 Comparison with Other Approaches

Criterion	GIFT	String Landscape	Lisi E_8
Falsifiable predictions	Yes (δ_{CP})	Limited	Limited
Continuous parameters	0	$\sim 10^{500}$	0
Discrete formula choices	33 (stat. constrained)	N/A	Fixed
Formal verification	Yes (Lean 4)	No	No
Precise predictions	32 at 0.24% ($+\delta_{CP}$ at 1σ)	Qualitative	Mass ratios

Distler–Garibaldi obstruction [35]: Lisi's E_8 theory attempted direct particle embedding, which is mathematically impossible. GIFT uses $E_8 \times E_8$ as algebraic scaffolding; particles emerge from cohomology, not representation decomposition.

Division algebra program (Furey [7], Baez [36]): Derives Standard Model gauge groups from division algebras. GIFT quantifies this relationship: $G_2 = \mathrm{Aut}(\mathbb{O})$ determines the holonomy, and $b_2 = \binom{7}{2} = 21$ gauge moduli arise from the 7 imaginary octonion units.

G_2 **manifold construction** (Crowley, Goette, Nordström [13]): Proves the moduli space of G_2 metrics is disconnected, with analytic invariant distinguishing components. This raises the selection question: which K_7 realizes physics? GIFT proposes that physical constraints select the manifold with $(b_2 = 21, b_3 = 77)$.

10.3 Limitations and Open Questions

Issue	Status
K_7 existence proof	Hypothesized, not explicitly constructed
Singularity structure	Required for non-abelian gauge groups, unspecified
$E_8 \times E_8$ selection principle	Input assumption
Formula selection rules	Statistically distinguished (Section 7.5), not derived
Dimensional quantities	Require scale determination (Sections 3 and 6)
Supersymmetry breaking	Not addressed
Hidden E_8 sector	Physical interpretation unclear
Quantum gravity completion	Not addressed

We do not claim to have solved these problems. The framework's value lies in producing falsifiable predictions from stated assumptions.

Formula selection: The principle selecting specific algebraic combinations remains unknown. However, exhaustive enumeration within a bounded grammar (Section 7.5) establishes three independent lines of evidence: (1) 12 of 17 GIFT formulas rank first by prediction error, (2) all pilot formulas occupy the Pareto frontier, and (3) combined null-model p-values of 10^{-11} reject accidental matching. Crucially, the non-optimal formulas (Section 7.5.7) provide evidence against post-hoc selection: GIFT trades per-observable optimality for cross-observable structural coherence. The deeper selection rule awaits discovery; possible approaches include variational principles on G_2 moduli space, calibrated geometry constraints, and K-theory classification.

Dimensionless vs running: GIFT predictions are dimensionless ratios derived from topology. The torsional geodesic framework (Section 3) provides the dynamical mechanism: geodesic flow on K_7 with torsion maps to RG evolution, with beta-functions as velocities and torsion as the interaction kernel. This addresses the question "at which energy scale?" for dimensional quantities. The 0.195% deviation in $\sin^2\theta_W$ may reflect radiative corrections (the topological ratio 3/13 corresponds to the $\overline{\text{MS}}$ value at M_Z; see S2 Section 11), experimental extraction procedure, or genuine discrepancy requiring framework revision.

10.4 Numerology Concerns

Integer arithmetic yielding physical constants invites skepticism. Our responses:

1. **Falsifiability**: If DUNE measures δ_{CP} outside $[182°, 212°]$, the framework fails regardless of arithmetic elegance.

2. **Statistical analysis**: The configuration $(21, 77)$ is the unique optimum among 3,070,396 tested (including 30 known G_2 manifolds), Pareto-optimal, not an arbitrary choice.

3. **Structural coherence**: Key quantities admit multiple equivalent algebraic formulations (14 for $\sin^2\theta_W$, 20 for Q_{Koide}) within the enumerated grammar, suggesting structural coherence rather than isolated coincidences.

4. **Formula-level selection**: Exhaustive enumeration within a bounded grammar (Section 7.5) shows GIFT formulas rank first or near-first. A joint null model yields $p < 1.5 \times 10^{-5}$ without independence assumptions; permutation tests yield $p < 6 \times 10^{-6}$; leave-one-out cross-validation confirms $(21, 77)$ as the unique optimum in 28/28 cases.

5. **Structural coherence over optimality**: Not all GIFT formulas rank #1 (Section 7.5.7). The non-optimal choices (θ_{13} at rank #10, λ_H at rank #7) reflect cross-observable structural constraints, not fitting: a cherry-picked numerology would select the best formula for each observable independently.

6. **Epistemic humility**: We present this as exploration, not established physics. Only experiment decides.

11 Conclusion

We have explored a framework deriving 33 dimensionless Standard Model parameters from topological invariants of a hypothesized G_2 manifold K_7 with $E_8 \times E_8$ gauge structure:

- **33 derived relations** with mean deviation **0.24%** across 32 well-measured observables (18 core + 15 extended; 0.57% including δ_{CP})
- **Formal verification** of arithmetic consistency (2400+ Lean 4 theorems, zero sorry, zero custom axioms)
- **Statistical uniqueness** of $(b_2, b_3) = (21, 77)$ at $> 4.2\sigma$ among 3,070,396 alternatives (including 30 known G_2 manifolds), Pareto-optimal, confirmed by Bayesian analysis (BF 288–4,567) and Westfall–Young correction (11/33 individually significant)
- **Formula-level selection**: Joint null model $p < 1.5 \times 10^{-5}$, permutation test $p < 6 \times 10^{-6}$, leave-one-out stability 28/28 (Section 7.5)
- **Torsional dynamics** connecting topology to RG flow via geodesic equations on K_7 (Section 3)
- **Scale determination**: Electron mass at 0.09% and electroweak scale at 0.4% from topological exponents (Section 6, status: THEORETICAL)
- **Falsifiable prediction** $\delta_{CP} = 197°$ (within 1σ of NuFIT 6.0 best-fit $177° \pm 20°$), testable by DUNE
- **Numerical G_2 metric program** with torsion scaling law $\nabla\varphi(L) = 8.46 \times 10^{-4}/L^2$ (unique global minimum), spectral fingerprint $[1, 10, 9, 30]$ at 5.8σ, G_2 Yukawa selection rule $Y(7 \times 7 \times 7) = 0$, and topological 3-form norm $|\varphi|^2 = 42$

We do not claim this framework is correct. It may represent:

(a) Genuine geometric insight

(b) Effective approximation

(c) Elaborate coincidence

Only experiment, particularly DUNE, can discriminate. The deeper question, why octonionic geometry would determine particle physics parameters, remains open. But the empirical success of 32 predictions at 0.24% mean deviation — with a 33rd (δ_{CP}) at 1σ from current data — derived from zero adjustable parameters and validated against 3 million alternative configurations, suggests that topology and physics may be more intimately connected than currently understood.

Acknowledgments

The mathematical foundations draw on work by Dominic Joyce, Alexei Kovalev, Mark Haskins, and collaborators on G_2 manifold construction. The standard associative 3-form φ_0 originates from Harvey and Lawson's foundational work on calibrated geometries. The Lean 4 verification relies on the Mathlib community's extensive formalization efforts. Experimental data come from the Particle Data Group, NuFIT collaboration, Planck collaboration, and DUNE technical design reports.

The octonion-Cayley connection and its role in G_2 structure benefited from insights in de-johannes/FirstDistinction. The blueprint documentation workflow follows the approach developed by math-inc/KakeyaFiniteFields.

Author's note

This framework was developed through sustained collaboration between the author and several AI systems, primarily Claude (Anthropic), with contributions from GPT (OpenAI), Gemini (Google), Grok (xAI), for specific mathematical insights. The formal verification in Lean 4, architectural decisions, and many key derivations emerged from iterative dialogue sessions over several months. This collaboration follows transparent crediting approach for AI-assisted mathematical research. Whether these algebraic relations reflect deep geometry or elaborate coincidence is an empirical question that depends on mathematical coherence and experimental accuracy, not on the means of discovery. Mathematics is evaluated on results, not résumés.

Data Availability

- Paper and data: https://doi.org/10.5281/zenodo.17979433
- Code: https://github.com/gift-framework/core
- Lean proofs: https://github.com/gift-framework/core/tree/main/Lean

Competing Interests

The author declares no competing interests.

References

[1] Particle Data Group, "Review of Particle Physics," *Phys. Rev. D* **110**, 030001 (2024).

[2] S. Weinberg, "Implications of dynamical symmetry breaking," *Phys. Rev. D* **13**, 974 (1976).

[3] Planck Collaboration, "Planck 2018 results. VI. Cosmological parameters," *Astron. Astrophys.* **641**, A6 (2020).

[4] A.G. Riess et al., "A comprehensive measurement of the local value of the Hubble constant," *ApJL* **934**, L7 (2022).

[5] C.D. Froggatt, H.B. Nielsen, "Hierarchy of quark masses, Cabibbo angles and CP violation," *Nucl. Phys. B* **147**, 277 (1979).

[6] Y. Koide, "Fermion-boson two-body model of quarks and leptons and Cabibbo mixing," *Lett. Nuovo Cim.* **34**, 201 (1982).

[7] C. Furey, "Standard Model physics from an algebra?" PhD thesis, University of Waterloo (2015).

[8] N. Furey, M.J. Hughes, "One generation of standard model Weyl representations as a single copy of $\mathbb{R} \otimes \mathbb{C} \otimes \mathbb{H} \otimes \mathbb{O}$," *Phys. Lett. B* **831**, 137186 (2022).

[9] R. Wilson, "E_8 and Standard Model plus gravity," arXiv:2404.18938 [hep-th] (2024, preprint).

[10] T.P. Singh et al., "An $E_8 \otimes E_8$ unification of the Standard Model with pre-gravitation," arXiv:2206.06911v3 (2024).

[11] B.S. Acharya, S. Gukov, "M-theory and singularities of exceptional holonomy manifolds," *Phys. Rep.* **392**, 121 (2004).

[12] L. Foscolo et al., "Complete non-compact G_2-manifolds from asymptotically conical Calabi–Yau 3-folds," *Duke Math. J.* **170**, 3 (2021).

[13] D. Crowley, S. Goette, J. Nordström, "An analytic invariant of G_2 manifolds," *Invent. Math.* **239**(3), 865–907 (2025).

[14] J. Nordström, "Extra-twisted connected sum G_2-manifolds," *Ann. Glob. Anal. Geom.* **64**, art. 2 (2023). arXiv:1809.09083.

[15] G. Bera, "New constructions of G_2-manifolds," arXiv:2209.00156 (2025).

[16] T. Dray, C.A. Manogue, *The Geometry of the Octonions*, World Scientific (2015).

[17] J.F. Adams, *Lectures on Exceptional Lie Groups*, University of Chicago Press (1996).

[18] D.J. Gross et al., "Heterotic string theory," *Nucl. Phys. B* **256**, 253 (1985).

[19] D.D. Joyce, *Compact Manifolds with Special Holonomy*, Oxford University Press (2000).

[20] A. Kovalev, "Twisted connected sums and special Riemannian holonomy," *J. Reine Angew. Math.* **565**, 125 (2003).

[21] A. Corti, M. Haskins, J. Nordström, T. Pacini, "G_2-manifolds and associative submanifolds via semi-Fano 3-folds," *Duke Math. J.* **164**, 1971 (2015).

[22] R. Harvey, H.B. Lawson, "Calibrated geometries," *Acta Math.* **148**, 47–157 (1982).

[23] B.S. Acharya, "M-theory, Joyce orbifolds and Super Yang–Mills," *Class. Quant. Grav.* **19**, 5619 (2002).

[24] B.S. Acharya, E. Witten, "Chiral fermions from manifolds of G_2 holonomy," arXiv:hep-th/0109152 (2001).

[25] T2K, NOvA Collaborations, "Joint oscillation analysis," *Nature* **646**(8086), 818–824 (2025). DOI: 10.1038/s41586-025-09599-3.

[26] NuFIT 6.0 Collaboration, "Global analysis of neutrino oscillations," www.nu-fit.org (2024).

[27] L. de Moura, S. Ullrich, "The Lean 4 theorem prover and programming language," CADE 28, 625 (2021).

[28] mathlib Community, "mathlib4: Mathematics in Lean 4," github.com/leanprover-community/mathlib4.

[29] DUNE Collaboration, "Long-baseline neutrino facility (LBNF) and Deep Underground Neutrino Experiment (DUNE) conceptual design report," FERMILAB-TM-2696 (2020).

[30] DUNE Collaboration, "Prospects for beyond the Standard Model physics searches," arXiv:2103.04797 (2021).

[31] E. Witten, "Strong coupling expansion of Calabi–Yau compactification," *Nucl. Phys. B* **471**, 135 (1996).

[32] B.S. Acharya et al., "An M-theory solution to the hierarchy problem," *Phys. Rev. D* **76**, 126010 (2007).

[33] M. Atiyah, E. Witten, "M-theory dynamics on a manifold of G_2 holonomy," *Adv. Theor. Math. Phys.* **6**, 1 (2002).

[34] G. Kane, *String Theory and the Real World*, Cambridge University Press (2017).

[35] J. Distler, S. Garibaldi, "There is no 'Theory of Everything' inside E_8," *Commun. Math. Phys.* **298**, 419 (2010).

[36] J.C. Baez, "Octonions and the Standard Model," math.ucr.edu/home/baez/standard/ (2020–2025).

[37] E. Heyes, E. Hirst, H.N. Sá Earp, T.S.R. Silva, "Neural and numerical methods for G_2-structures on contact Calabi–Yau 7-manifolds," arXiv:2602.12438 (2026).

Appendix A: Topological Input Constants

Symbol	Definition	Value
$\dim(\mathrm{E}_8)$	Lie algebra dimension	248
$\mathrm{rank}(\mathrm{E}_8)$	Cartan subalgebra dimension	8
$\dim(K_7)$	Manifold dimension	7
$b_2(K_7)$	Second Betti number	21
$b_3(K_7)$	Third Betti number	77
$\dim(\mathrm{G}_2)$	Holonomy group dimension	14
$\dim(J_3(\mathbb{O}))$	Jordan algebra dimension	27

Appendix B: Derived Structural Constants

Symbol	Formula	Value
p_2	$\dim(\mathrm{G}_2)/\dim(K_7)$	2
Weyl	Pentagonal index: $(\dim(\mathrm{G}_2)+1)/N_{\mathrm{gen}}$	5
N_{gen}	Index theorem	3
H^*	b_2+b_3+1	99
τ	$(496\times 21)/(27\times 99)$	3472/891
κ_T	$1/(b_3-\dim(\mathrm{G}_2)-p_2)$	1/61
$\det(g)$	$p_2+1/(b_2+\dim(\mathrm{G}_2)-N_{\mathrm{gen}})$	65/32

Appendix C: Supplement Reference

Supplement	Content	Location
S1: Foundations	E_8, G_2, K_7 construction details	GIFT_v3.3_S1_foundations.md
S2: Derivations	Complete proofs of 18 relations	GIFT_v3.3_S2_derivations.md